



Magnesium sulfate inhibits binding of lipopolysaccharide to THP-1 cells by reducing expression of cluster of differentiation 14

Ya-Ying Chang^{1,2} · Tzu-Yu Lin^{2,3} · Ming-Chang Kao^{4,5} · Tsung-Ying Chen^{5,6} · Ching-Feng Cheng^{1,7} · Chih-Shung Wong⁸ · Chun-Jen Huang^{9,10}

Received: 6 November 2018 / Accepted: 18 January 2019 / Published online: 5 February 2019
© Springer Nature Switzerland AG 2019

Abstract

We investigated effects of magnesium sulfate (MgSO_4) on modulating lipopolysaccharide (LPS)–macrophage binding and cluster of differentiation 14 (CD14) expression. Flow cytometry data revealed that the mean levels of LPS–macrophage binding and membrane-bound CD14 expression (mCD14) in differentiated THP-1 cells (a human monocytic cell line) treated with LPS plus MgSO_4 (the LPS + M group) decreased by 28.2% and 25.3% compared with those THP-1 cells treated with LPS only (the LPS group) ($P < 0.001$ and $P = 0.037$), indicating that MgSO_4 significantly inhibits LPS–macrophage binding and mCD14 expression. Notably, these effects of MgSO_4 were counteracted by L-type calcium channel activation. Moreover, the mean level of soluble CD14 (sCD14; proteolytic cleavage product of CD14) in the LPS + M group was 25.6% higher than in the LPS group ($P < 0.001$), indicating that MgSO_4 significantly enhances CD14 proteolytic cleavage. Of note, serine protease inhibition mitigated effects of MgSO_4 on both decreasing mCD14 and increasing sCD14. In conclusion, MgSO_4 inhibits LPS–macrophage binding through reducing CD14 expression. The mechanisms may involve antagonizing L-type calcium channels and activating serine proteases.

Keywords CD14 · MgSO_4 · Calcium · L-type calcium channels · Protease

✉ Chun-Jen Huang
huangcj1112@gmail.com

- ¹ Institute of Medical Sciences, College of Medicine, Tzu Chi University, Hualien, Taiwan
- ² Department of Anesthesiology, Far Eastern Memorial Hospital, New Taipei City, Taiwan
- ³ Department of Mechanical Engineering, Yuan Ze University, Taoyuan, Taiwan
- ⁴ Department of Anesthesiology, Taipei Tzu Chi Hospital, New Taipei City, Taiwan
- ⁵ School of Medicine, College of Medicine, Tzu Chi University, Hualien, Taiwan
- ⁶ Departments of Anesthesiology, Hualien Tzu Chi Hospital, Hualien, Taiwan
- ⁷ Department of Pediatrics, Hualien Tzu Chi Hospital, Hualien, Taiwan
- ⁸ Department of Anesthesiology, Cathay General Hospital, Taipei, Taiwan
- ⁹ Department of Anesthesiology, Wan Fang Hospital, Taipei Medical University, Taipei, Taiwan
- ¹⁰ Graduate Institute of Clinical Medicine, College of Medicine, Taipei Medical University, Taipei, Taiwan

Introduction

Lipopolysaccharide (LPS) is a component of the outer membrane of gram-negative bacterial cells. Binding of LPS to the toll-like receptor 4 (TLR4) expressed in macrophages can elicit inflammatory responses. LPS is introduced to cluster of differentiation 14 (CD14) on the cell surface by LPS-binding protein. Subsequently, CD14 transfers LPS to TLR4 and initiates downstream inflammatory signaling cascades (Molteni et al. 2016; Park and Lee 2013; Rosadini and Kagan 2017). Alterations in CD14 levels regulate the capacity of endotoxin recognition as well as responsive inflammatory reactions. In clinical settings, elevated CD14 expression has been associated with multiple diseases and conditions, including sepsis, coronary artery disease, or hepatic ischemia–reperfusion injury (Cai et al. 2013; Chen et al. 2018; Lee et al. 2015). CD14 inhibition has been demonstrated to be a promising therapeutic strategy for some inflammatory diseases (Ma et al. 2013; Wei et al. 2018). CD14 exists either as a membrane-associated glycosylphosphatidylinositol-anchored protein on the surface of the immune cells (i.e., membrane-bound CD14, mCD14) or as a soluble protein (i.e., soluble CD14, sCD14) in the

supernatants. sCD14 is known to be derived from proteolytic cleavage of mCD14 (i.e., CD14 shedding) on the cell surface (Pham 2008). The enzymes mediating the proteolytic cleavage of mCD14 include some serine proteases and metalloproteinases. A decrease in levels of mCD14 has been demonstrated to cause reduced responsiveness to LPS and reduced cytokine production (Le-Barillec et al. 1999, 2000; Senft et al. 2005; Sugawara et al. 2000; Tada et al. 2002).

Magnesium sulfate (MgSO_4), a natural calcium antagonist and a potent L-type calcium channel inhibitor (Sonna et al. 1996), is used widely in clinical settings. For example, MgSO_4 exerts therapeutic effects on patients with asthma through bronchodilation (Kew et al. 2014). In addition, MgSO_4 exhibits potent anti-inflammatory effects and prevents LPS-induced organ injuries (Ahmed 2012; El-Tanbouly et al. 2015). MgSO_4 inhibits the upregulation of proinflammatory cytokines, such as tumor necrosis factor- α and interleukin- 1β . The mechanisms underlying the inhibitory effect of MgSO_4 on LPS-induced cytokine upregulation include inhibition of the transcription factor nuclear factor- κB (NF- κB) (Gao et al. 2013; Sugimoto et al. 2012). Because the binding of LPS to TLR4 on the cell surface can trigger NF- κB activation (Molteni et al. 2016; Park and Lee 2013; Rosadini and Kagan 2017), MgSO_4 is likely to act by inhibiting LPS–macrophage binding, thus exerting potent anti-inflammatory effects. To date, the effects of MgSO_4 on regulating the binding of LPS to macrophages have not been investigated.

In this study, we clarified whether MgSO_4 modulates LPS–macrophage binding and CD14 expression. We used a human monocytic leukemia cell line, THP-1 cells, for this study. The binding of LPS to immune cells was reported to be CD14-dependent (Troelstra et al. 1997). In addition, enhanced expression of CD14 has been reported in rats with magnesium-deficient diets (Chmielinska et al. 2005; Weglicki et al. 2010). On the basis of these data, we hypothesized that MgSO_4 reduces LPS binding to macrophages through the downregulation of CD14 expression. We also clarified whether the effect of MgSO_4 on CD14 expression was mediated through the proteolytic cleavage of CD14. Furthermore, our previous study showed that MgSO_4 exerts anti-inflammatory effects by antagonizing L-type calcium channels (Lin et al. 2010). Therefore, the involvement of the L-type calcium channels in the effects of MgSO_4 on LPS–macrophage binding and CD14 expression were investigated in this study.

Materials and methods

Cell culture

THP-1 cells (American Type Culture Collection, Manassas, VA, USA) were cultured in Roswell Park Memorial

Institute 1640 medium (Sigma-Aldrich, St. Louis, MO, USA) supplemented with 10% fetal bovine serum and 1% penicillin–streptomycin (Life Technologies, Carlsbad, CA, USA); the cells were incubated in a humidified chamber at 37 °C in a mixture of 95% air and 5% CO_2 . The THP-1 cells were differentiated into macrophages with phorbol myristate acetate (50 nM; Invivogen, San Diego, CA, USA) for 24 h, followed by overnight resting in fresh culture medium. Then the adherent differentiated THP-1 cells were harvested and employed in this study. Cells that had undergone fewer than 15 passages were used in this experiment.

Cell activation and experimental protocols

According to previously published protocols using THP-1 cells, we chose LPS (1 $\mu\text{g}/\text{mL}$, *Escherichia coli* Serotype 0127:B8 endotoxin; Sigma-Aldrich) to induce cell activation (Ma et al. 2017; Prestigiacomo et al. 2017). In this study, the THP-1 cells were treated with LPS only or LPS plus MgSO_4 (0.2 mM, 2 mM, 20 mM, or 200 mM, Sigma-Aldrich), and were denoted as the LPS, LPS + M0.2, LPS + M2, LPS + M20, and LPS + M200 groups, respectively. THP-1 cells were treated with MgSO_4 30 min before LPS treatment. Another two sets of THP-1 cells were treated with phosphate-buffered saline (PBS, Sigma-Aldrich; denoted as the PBS group) or MgSO_4 (0.2 mM, 2 mM, 20 mM, or 200 mM, Sigma-Aldrich; denoted as the M0.2, M2, M20, and M200 groups, respectively) and served as the control for vehicle and drug, respectively. In addition, an L-type calcium channel activator, Bay-K8644 (2 μM ; Sigma-Aldrich), was used to study the involvement of L-type calcium channels. The cells were treated with Bay-K8644 10 min before the MgSO_4 treatment. A mixed serine protease inhibitor (phenylmethanesulfonyl fluoride, PMSF, 0.4 mM; Sigma-Aldrich) and a metalloprotease inhibitor (ethylene glycol tetraacetic acid, EGTA, 1 mM; Sigma-Aldrich) were used to study the possible involvement of proteases and metalloproteinases, respectively. PMSF or EGTA was added 30 min before the administration of MgSO_4 .

MTT assay

The THP-1 cells were seeded in 96-well plates and incubated with LPS (1 $\mu\text{g}/\text{mL}$) with or without MgSO_4 . Cell viability was assayed using the MTT (3-(4,5-dimethylthiazol-2-yl)-2,5-diphenyltetrazolium bromide) assay. A commercial kit (Cell Proliferation Kit I, Sigma-Aldrich) was employed and the MTT assay was performed according to the manufacturer's protocols. Levels of cell viability were reported as the ratio of each studied group to the PBS group.

Flow cytometry

Flow cytometry protocols for assaying LPS binding to macrophages and surface expression of mCD14 were adapted from our previous report (Chen et al. 2012). To assay the binding of LPS, the THP-1 cells were incubated with LPS conjugated with fluorescein isothiocyanate (FITC-LPS, 1 µg/mL, Sigma-Aldrich) at 37 °C, which is the optimal temperature for most enzymes. For assaying surface expression of mCD14, cells were stained using a CD14 antibody (Alexa Fluor 488 Mouse Anti-human CD14, BD Sciences, Franklin Lakes, NJ, USA). Samples were collected and analyzed using a fluorescence-activated cell sorting flow cytometer (Cytomic FC50 Flow Cytometer; Beckman Coulter, Inc., Fullerton, CA, USA). The signal of the isotype control (Alexa Fluor 488 Mouse IgG2b, BD) was used as the background binding and was subtracted from the respective antibody expression. The mean fluorescence intensity (MFI) was measured to assay the binding of FITC-LPS to THP-1 cells and was reported as the ratio of each studied group to the PBS group. The levels of mCD14 were measured using the positively stained events, and the levels were expressed as the ratio of CD14-positive events in each studied group to those in the PBS group.

Immunofluorescence microscopy

Immunofluorescence microscopy was also performed to assay the binding of FITC-LPS to the THP-1 cells. The THP-1 cells were seeded onto glass coverslips placed at the bottom of the wells of six-well plates and were incubated with FITC-LPS (1 µg/mL) for 60 min. Then cells were fixed with 4% paraformaldehyde without permeabilization. After washing with PBS, the nuclei were counterstained using diamidino-2-phenylindole (Pierce). The coverslips were then mounted using mounting medium (Sigma-Aldrich) and imaged through immunofluorescence microscopy (Nuance FX, CRi, Woburn, MA, USA). The cellular fluorescence strength was determined by drawing circles around 15 cells representative from at least three different fields in each group. Then the fluorescence intensity per cell was reported according to the mean fluorescence value in the green histogram using ImageJ software freely available at <http://rsb.info.nih.gov/ij/>.

RNA extraction and real-time polymerase chain reaction (PCR)

Transcriptional expression of CD14 was quantified by real-time PCR according to a previously published protocol (Zhu et al. 2014). In brief, total RNA of THP-1 cells were extracted and purified (Trizol reagent, Invitrogen). After reverse-transcription to cDNA, real-time PCR measurement

was then performed using iTaq Universal SYBR Green Supermix (Bio-Rad Laboratories, Hercules, CA, USA) and a CFX96 real-time PCR instrument (Bio-Rad). The following primers were used: CD14 5'-GGGACTTGGATTTGG TGGCA-3' and 3'-GCCCCCTTCCTTTCCTTATATCC-5' (Shin et al. 2015); GAPDH 5'-AGAAGGCTGGGGCTC ATTTG-3' and 3'-AGGGGCCATCCACAGTCTTC-5'. Each sample was run in triplicate. Transcriptional expression of CD14 was normalized to GAPDH using the standard curve method. Levels of CD14 mRNA were reported as the ratio of each studied group to the PBS group.

Immunoblotting assay

The THP-1 cells were seeded in 10-cm dishes (cell density approximately 10⁶ cells/mL) and were treated as described previously. After treatment, the cells were lysed in radioimmunoprecipitation assay buffer containing 1:100 protease inhibitors (both from Sigma-Aldrich). The protein levels in the cell lysates were then determined by bicinchoninic acid assay (protein assay kit, Pierce). The samples from the cell lysates were loaded onto sodium dodecyl sulfate polyacrylamide gels and subjected to electrophoresis. Subsequently, the separated proteins were transferred to nitrocellulose membranes (Bio-Rad). After blocking with 5% non-fat milk, the membranes were incubated with a primary antibody against CD14 (1:200 dilution, Santa Cruz, CA, USA) or actin (as an internal standard; 1:5000 dilution; Millipore Corporation, Burlington, MA, USA) and then with a secondary antibody (horseradish peroxidase-conjugated anti-mouse IgG antibody, Amersham Pharmacia Biotech, Inc., Piscataway, NJ, USA). The protein bands were then visualized through chemiluminescence (ECL plus kit; Amersham) and quantified using ImageJ software.

Enzyme-linked immunosorbent assay (ELISA)

The cells were treated with LPS (1 µg/mL) with or without MgSO₄. Then, the supernatants of the cell cultures were harvested and the levels of IL-1β and sCD14 in the supernatants were quantified using commercial ELISA kits (ELISA kits for human IL-1β and human sCD14; R&D Systems, Minneapolis, MN, USA), as per the manufacturer's protocols.

Measurement of intracellular calcium levels

The levels of intracellular calcium were measured using a commercial kit according to the manufacturer's protocol (FLUOFORTE calcium assay kit, Enzo Life Sciences Inc., Farmingdale, NY, USA). After treatment, as previously described, the THP-1 cells were harvested, pelleted, mixed with the FLUOFORTE dye solution, and loaded for analysis. The levels of intracellular calcium were measured

every minute using a fluorometric imaging plate reader ($E_x = 490$ nm and $E_m = 525$ nm; Promega Corp., Madison, WI, USA) for 60 min. The intracellular calcium levels in each group before treatment were measured and used as the baseline. The ratio of fluorescence to baseline (fluorescence) in each group for each minute was calculated, and the ratios of fluorescence in each group at 60 min after LPS stimulation or at a compatible time point in groups without LPS stimulation were compared.

Statistical methods

Data were analyzed through one-way analysis of variance with Tukey's test, as the post hoc test, to determine the between-group differences. Data were expressed as mean \pm standard deviation, and $P < 0.05$ was considered statistically significant. A commercial software package (SigmaStat for Windows; SPSS Science, Chicago, IL, USA) was used for data analysis.

Results

Cell viability

Cell viability was measured by MTT assay and shown in Fig. 1a ($n = 5$ in each group). The MTT assay data revealed that the cell viabilities of the PBS, M0.2, M2, M20, LPS, LPS + M0.2, LPS + M2, and LPS + M20 groups were not significantly different. However, cell viabilities of the M200 and LPS + M200 groups were significantly lower than the PBS group (both $P < 0.001$). On the basis of these data, the

200 mM dose of $MgSO_4$ was excluded from the following experiments.

$MgSO_4$ reduced IL-1 β release

THP-1 cells were allocated to the PBS, M20, LPS, LPS + M0.2, LPS + M2, or LPS + M20 group ($n = 5$ in each group). Levels of IL-1 β were assayed by ELISA and illustrated in Fig. 1b. IL-1 β concentrations in the PBS and M20 groups were low. In contrast, the IL-1 β concentration in the LPS group was significantly higher than those in the PBS and the LPS + M20 groups (both $P < 0.001$). Of note, the differences in IL-1 β concentrations between the LPS, LPS + M0.2, and LPS + M2 groups were not statistically significant.

$MgSO_4$ reduced LPS binding

Next, we chose to use 20 mM $MgSO_4$ to investigate the effects of $MgSO_4$ on LPS recognition and CD14 expression. Figure 2a illustrates the flow cytometry data of FITC-LPS binding to the THP-1 cells. The THP-1 cells were harvested at 30, 60, and 120 min after incubation with FITC-LPS or at compatible time points in groups without FITC-LPS ($n = 6$ in each group). Our data revealed that the MFI ratios at all time points in the PBS and M20 groups did not differ significantly. Notably, the 30-, 60-, and 120-min MFI ratios in the LPS group were significantly higher than those in the PBS group (all $P < 0.001$). The 30-min MFI ratio in the LPS + M20 group was not significantly different from that in the LPS group, whereas the 60- and 120-min MFI ratios in the LPS + M20 group were significantly lower than those

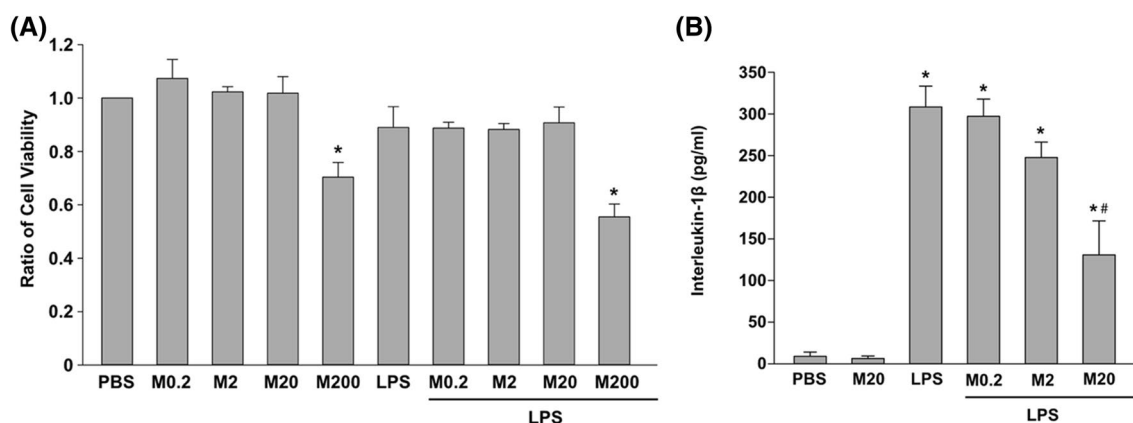


Fig. 1 Effects of magnesium sulfate ($MgSO_4$) on cell viability and interleukin-1 β (IL-1 β) release. **a** Cell viability was measured by MTT assay and expressed as the ratio of each studied group to the phosphate-buffered saline (PBS) group. **b** Concentrations of IL-1 β in the supernatants were assayed by enzyme-linked immunosorbent assay. PBS, the phosphate-buffered saline group; M0.2, the $MgSO_4$ (0.2 mM) group; M2, the $MgSO_4$ (2 mM) group; M20, the

$MgSO_4$ (20 mM) group; M200, the $MgSO_4$ (200 mM) group; LPS, the lipopolysaccharide (1 μ g/mL) group; LPS + M0.2, the LPS plus $MgSO_4$ (0.2 mM) group; LPS + M2, the LPS plus $MgSO_4$ (2 mM) group; LPS + M20, the LPS plus $MgSO_4$ (20 mM) group; LPS + M200, the LPS plus $MgSO_4$ (200 mM) group. Data are presented as mean \pm standard deviation ($n = 5$ in each group). * $P < 0.05$ versus the PBS group, ** $P < 0.05$ versus the LPS group

in the LPS group (both $P < 0.001$). The mean 60-min MFI ratio in the LPS group was 28.2% higher than that in the LPS + M20 group. The histogram data paralleled the MFI ratio data. A representative 60-min histogram is illustrated in Fig. 2a.

The binding of FITC-LPS to the THP-1 cells at 60 min after LPS stimulation or at the comparable time point in the groups without LPS stimulation was imaged through immunofluorescence microscopy (Fig. 2b). The immunofluorescence signals in the PBS and M20 groups were extremely

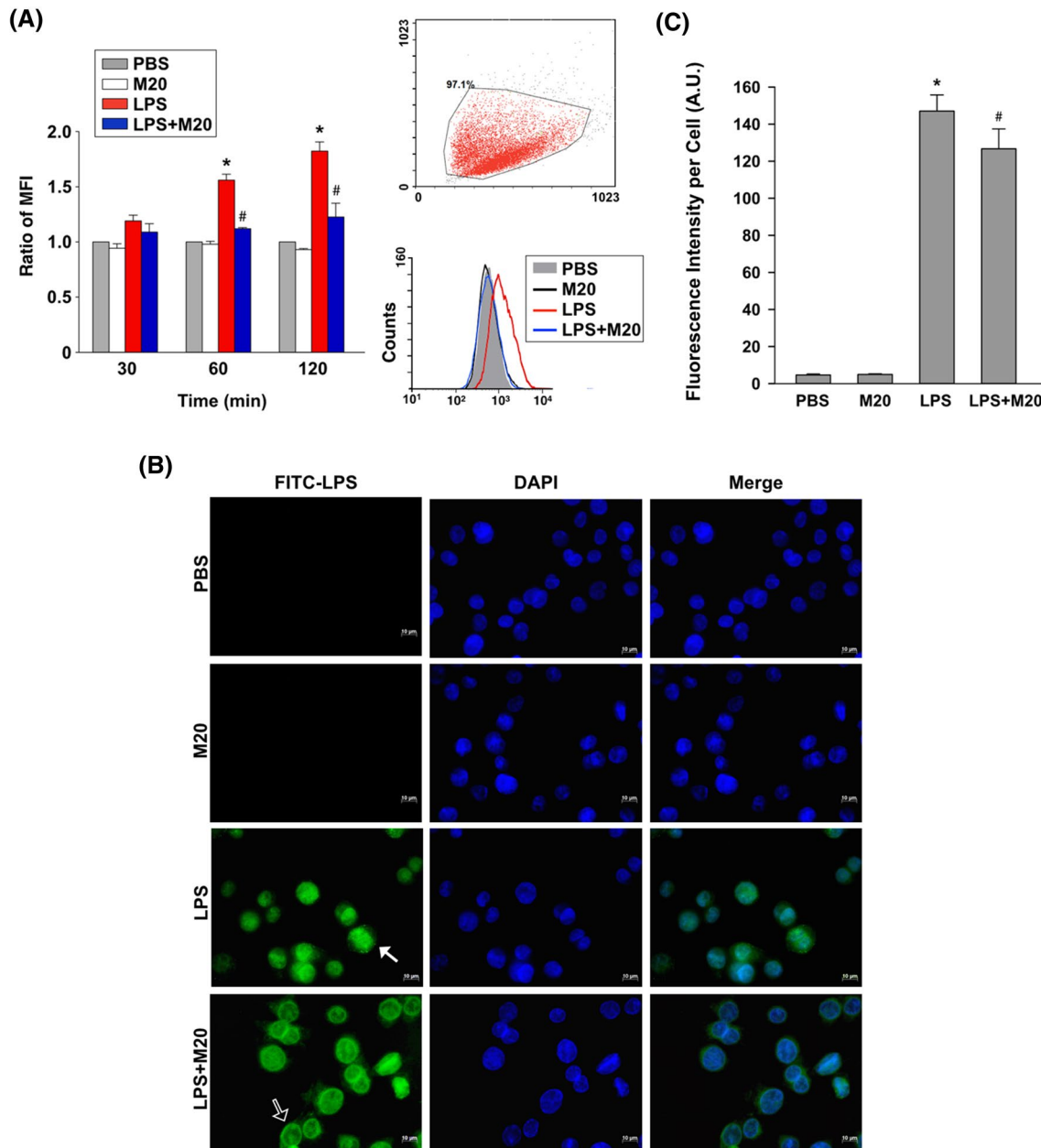


Fig. 2 Effect of magnesium sulfate (MgSO_4) on lipopolysaccharide (LPS)–macrophage binding. **a** Binding of LPS conjugated with fluorescein isothiocyanate (FITC-LPS) to the THP-1 cells at indicated time points was quantified through flow cytometry. The mean fluorescence intensity (MFI) ratio in each group was compared with that in the phosphate-buffered saline (PBS) group and expressed as ratio of MFI. A representative 60-min histogram is also illustrated. **b** Binding of FITC-LPS to the THP-1 cells at 60 min after LPS stimulation or at the comparable time point in groups without LPS stimulation

was imaged through immunofluorescence microscopy. **c** Quantitative assay of the fluorescence intensity per cell at 60 min after LPS stimulation or at the comparable time point in groups without LPS stimulation. PBS, the phosphate-buffered saline group; M20, the MgSO_4 (20 mM) group; LPS, the lipopolysaccharide (1 $\mu\text{g}/\text{mL}$) group; LPS + M20, LPS plus MgSO_4 (20 mM); DAPI, 4',6-diamidino-2-phenylindole. Data are presented as mean \pm standard deviation ($n=6$ in each group). * $P < 0.05$ for the LPS group versus the PBS group, # $P < 0.05$ for the LPS + M20 group versus the LPS group

low and almost undetectable (Fig. 2b). The immunofluorescence signals in the LPS group were evidently high. Most cells in the LPS group were positively stained with FITC-LPS (solid arrow in Fig. 2b), as evidently high fluorescence intensity was observed. However, the immunofluorescence signal in the LPS + M20 group was comparatively weak (hollow arrow in Fig. 2b). The quantitative results showed that the fluorescence intensity per cell in the LPS group was significantly higher than in the PBS group ($P < 0.001$; Fig. 2c) and that in the LPS + M20 group was significantly lower than in the LPS group ($P < 0.001$; Fig. 2c).

MgSO₄ reduced CD14 upregulation

On the basis of the data of FITC-LPS binding to the THP-1 cells, we used 60 min of LPS stimulation for the remaining experiments. Levels of CD14 mRNA were measured by real-time PCR ($n = 5$ in each group) and illustrated in Fig. 3a. Our data revealed that the CD14/GAPDH ratios in the PBS and M20 group were not significantly different. Of note, the CD14/GAPDH ratio in the LPS group was significantly higher than that in the PBS group ($P < 0.001$). MgSO₄ treatment significantly reduced the CD14/GAPDH ratio induced by LPS ($P = 0.049$, the LPS + M20 group versus the LPS group).

Levels of CD14 protein were measured using immunoblotting assay (Fig. 3b, $n = 4$ in each group). Densitometric data revealed that the CD14 protein band densities in the cell lysates of the PBS and M20 groups were comparable (0.627 ± 0.0643 versus 0.533 ± 0.0577 , $P = 0.428$). The CD14 protein band density in the LPS group (0.847 ± 0.0874) was significantly higher than that in the PBS group ($P = 0.022$). Similarly, the CD14 protein band density in the LPS + M20 group (0.520 ± 0.0721) was significantly lower than that in the LPS group ($P = 0.002$).

Expression of mCD14 was measured by flow cytometry (Fig. 3c, $n = 5$ in each group). The ratios of CD14-positive events in the PBS and M20 groups were not significantly different. The ratio of CD14-positive events in the LPS group was significantly higher than that in the PBS group ($P = 0.024$). In addition, MgSO₄ treatment reduced the mean levels of LPS-upregulated mCD14 by 25.3% ($P = 0.037$, the LPS + M20 group versus the LPS group). The histogram data paralleled the data of the ratios of CD14-positive events (Fig. 3c).

MgSO₄ increased CD14 shedding

Levels of sCD14 in the supernatants were measured by ELISA (Fig. 3d, $n = 6$ in each group). We found that the sCD14 level in the LPS group was significantly higher than that in the PBS group ($P < 0.001$). Contrasting the data of mCD14 expression levels in response to MgSO₄ treatment,

the mean sCD14 level in the LPS + M20 group was 25.6% higher than in the LPS group ($P < 0.001$). The sCD14 levels in the PBS and M20 groups were comparable.

Activation of L-type calcium channels counteracted the effects of MgSO₄ on LPS binding and CD14 upregulation but not CD14 shedding

Because MgSO₄ is an L-type calcium channel antagonist, we examined the possible roles of the L-type calcium channels in mediating the aforementioned effects of MgSO₄. THP-1 cells were allocated to receive LPS (1 $\mu\text{g}/\text{mL}$), LPS plus MgSO₄ (20 mM), or LPS plus MgSO₄ (20 mM) plus Bay-K8644 (2 μM) and denoted as the LPS, LPS + M20, and LPS + M20 + K8644 group, respectively. The THP-1 cells were harvested at 60 min after stimulation with LPS ($n = 4$ in each group). Our data revealed that the MFI ratio in the LPS + M20 + K8644 group was significantly higher than that in the LPS + M20 group ($P < 0.001$, Fig. 4a). The ratio of CD14-positive events in the LPS + M20 + K8644 group was also significantly higher than that in the LPS + M20 group (Fig. 4b; $P < 0.001$). However, sCD14 levels in the supernatants did not differ significantly between the LPS + M20 and LPS + M20 + K8644 groups (Fig. 4c).

Changes in intracellular calcium levels

Levels of intracellular calcium were measured using a FLUOFORTE calcium assay kit. Figure 5a shows the ratios of fluorescence to the baseline in each group measured every minute over 60 min of LPS stimulation or comparable duration in groups without LPS stimulation ($n = 5$ in each group). Our data revealed that the ratios of fluorescence in the PBS and M20 groups did not increase significantly over 60 min. By contrast, in the LPS, LPS + M20, and LPS + M20 + K8644 groups, significant increases were observed in the ratios of fluorescence over 60 min of LPS stimulation. Notably, the magnitude of increase in the ratios of fluorescence in the LPS + M20 group was lower than those in the LPS and LPS + M20 + K8644 groups. In addition, the ratios of fluorescence in each group at 60-min of LPS stimulation or at a comparable time point in groups without LPS stimulation were compared (Fig. 5b, $n = 5$ in each group). The ratios of fluorescence in the PBS and M20 groups were low. The ratio of fluorescence in the LPS group was significantly higher than that in the PBS group ($P < 0.001$). By contrast, the ratio of fluorescence in the LPS + M20 group was significantly lower than the ratios in the LPS and LPS + M20 + K8644 groups (both $P < 0.001$).

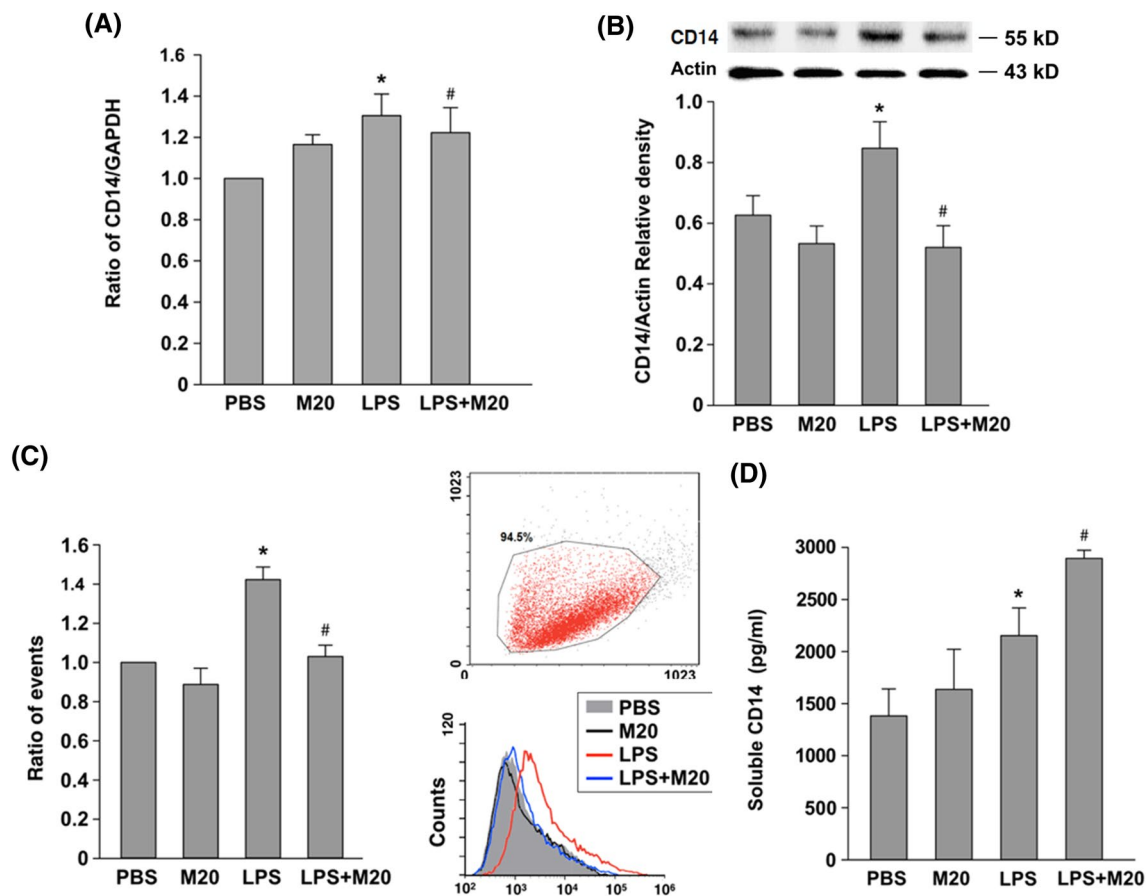


Fig. 3 Effect of magnesium sulfate (MgSO_4) on cluster of differentiation 14 (CD14) expression. **a** CD14 mRNA levels in the cell lysates of the THP-1 cells at 60 min after lipopolysaccharide (LPS) stimulation or at a comparable time point in groups without LPS stimulation were measured by real-time polymerase chain reaction. GAPDH was used as the internal control ($n=5$ in each group). The levels of CD14 mRNA were normalized to the levels of GAPDH in each studied group and reported as the ratio to the phosphate-buffered saline (PBS) group. **b** CD14 protein levels in the cell lysates were measured by immunoblotting assay ($n=5$ in each group). Representative gel photography and relative densitometry data are shown. **c** Expression

of membrane-bound CD14 was measured by flow cytometry. Data from each group were compared with those of the PBS group and are expressed as the ratio of CD14-positive events. **d** Levels of soluble CD14 were measured by enzyme-linked immunosorbent assay ($n=6$ in each group). PBS, the phosphate-buffered saline group; M20, the MgSO_4 (20 mM) group; LPS, the lipopolysaccharide (1 $\mu\text{g}/\text{mL}$) group; LPS+M20, the LPS plus MgSO_4 (20 mM) group. Data are presented as mean \pm standard deviation. * $P < 0.05$ for the LPS group versus the PBS group, # $P < 0.05$ for the LPS+M20 group versus the LPS group

Inhibition of serine proteases but not metalloproteinases mitigated the effect of MgSO_4 on LPS-macrophage binding, CD14 upregulation, and CD14 shedding

We examined the role of serine protease or metalloproteinase in mediating the effects of MgSO_4 on LPS-macrophage binding and CD14 expression. THP-1 cells were allocated to receive LPS (1 $\mu\text{g}/\text{mL}$), LPS plus MgSO_4 (20 mM), LPS plus MgSO_4 (20 mM) plus PMSF (0.4 mM), or LPS plus MgSO_4 (20 mM) plus EGTA (1 mM) and denoted as the LPS, LPS + M20, LPS + M20 + PMSF, and LPS + M20 + EGTA group, respectively ($n=6$ in each

group). Our data revealed that the MFI ratio (Fig. 6a) and the ratio of CD14-positive events (Fig. 6b) in the LPS + M20 + PMSF group were significantly higher than that in the LPS + M20 group ($P=0.006$ and $=0.017$), whereas the sCD14 level in the LPS + M20 + PMSF group was significantly lower than that in the LPS + M20 group (Fig. 6c; $P=0.015$). In contrast, the ratio of MFI, the ratio of CD14-positive events, or the sCD14 levels did not differ significantly between the LPS + M20 and LPS + M20 + EGTA groups (Fig. 6a–c). These results suggested that serine protease, but not metalloproteinases, is involved in mediating the effect of MgSO_4 on modulating LPS-macrophage binding and CD14 expression.

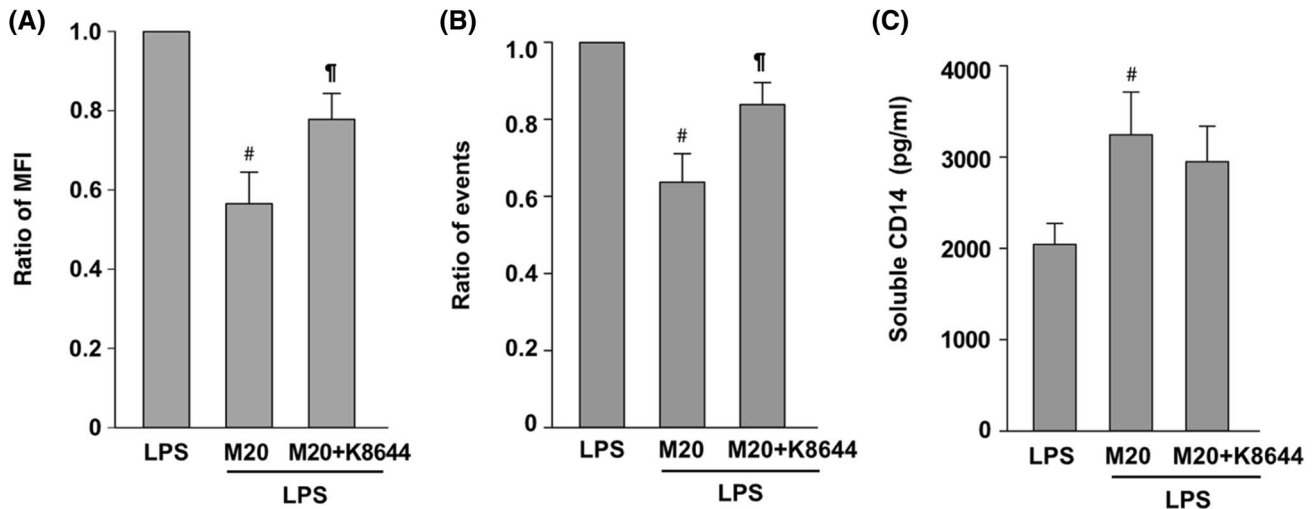


Fig. 4 L-type calcium channel activation counteracting effects of magnesium sulfate (MgSO_4) on modulating lipopolysaccharide (LPS)–macrophage binding and cluster of differentiation 14 (CD14) expression. **a** Binding of LPS to macrophages at 60 min after incubation with fluorescein isothiocyanate-conjugated LPS (FITC-LPS) was measured by flow cytometry. Data from each group were compared with that from the lipopolysaccharide (LPS) group and are expressed as the ratio of mean fluorescence intensity (MFI). **b** Expression of membrane-bound CD14 at 60 min after LPS stimulation was measured by flow cytometry. Data from each group were compared with

that from the lipopolysaccharide (LPS) group and are expressed as the ratio of CD14-positive events. **c** Levels of soluble CD14 at 60 min after LPS stimulation were measured by enzyme-linked immunosorbent assay. LPS, the lipopolysaccharide (1 $\mu\text{g}/\text{mL}$) group; LPS + M20, the LPS plus MgSO_4 (20 mM) group; LPS + M20 + K8644, the LPS plus MgSO_4 (20 mM) plus Bay-K8644 (an L-type calcium channel activator, 2 μM) group. Data are presented as mean \pm standard deviation ($n=4$ in each group). # $P < 0.05$ for the LPS + M20 group versus the LPS group, ¶ $P < 0.05$ for the LPS + M20 + K8644 group versus the LPS + M20 group

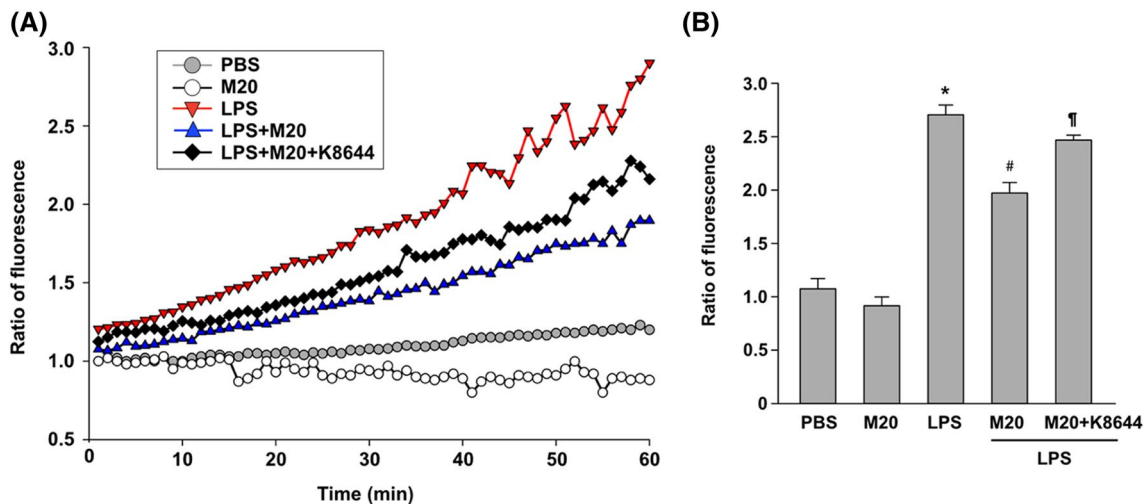


Fig. 5 Changes in intracellular calcium levels. **a** Levels of intracellular calcium were measured using a FLUOFORTE calcium assay kit. The ratios of fluorescence to baseline in each group were measured and plotted for every minute. **b** Ratios of fluorescence to baseline in each group at 60 min of lipopolysaccharide (LPS) stimulation or at a comparable time point in groups without LPS stimulation were compared. PBS, the phosphate-buffered saline group; M20, the MgSO_4

(20 mM) group; LPS, the LPS (1 $\mu\text{g}/\text{mL}$) group; LPS + M20, the LPS plus MgSO_4 (20 mM) group; LPS + M20 + K8644, the LPS plus MgSO_4 (20 mM) plus Bay-K8644 (2 μM) group. Data are presented as mean \pm standard deviation ($n=5$ in each group). * $P < 0.05$ for the LPS group versus the PBS group, # $P < 0.05$ for the LPS + M20 group versus the LPS group, ¶ $P < 0.05$ for the LPS + M20 + K8644 group versus the LPS + M20 group

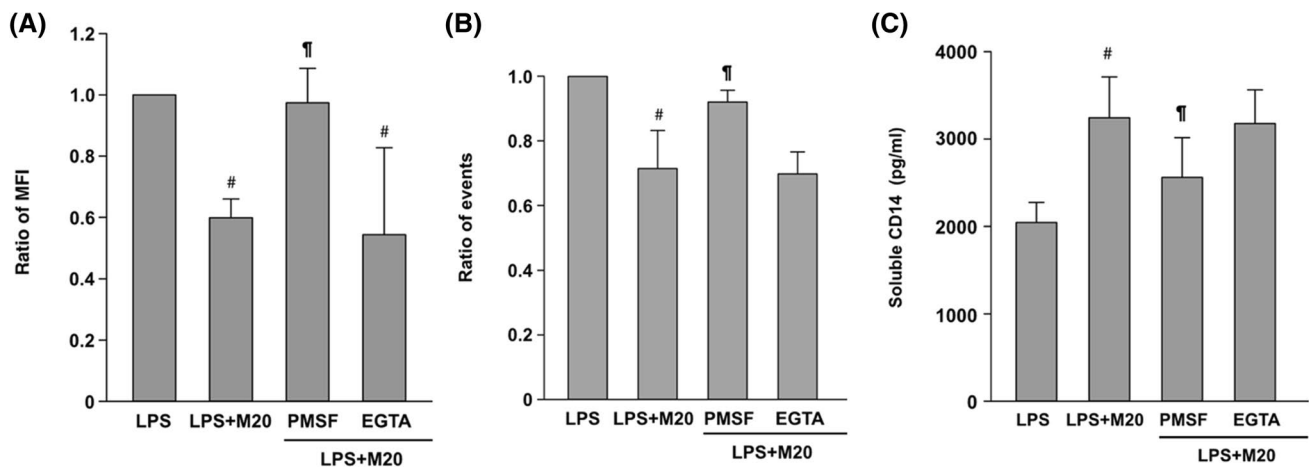


Fig. 6 Proteolysis inhibition counteracting effects of magnesium sulfate (MgSO_4) on modulating lipopolysaccharide (LPS)–macrophage binding and cluster of differentiation 14 (CD14) expression. **a** Binding of LPS to macrophages at 60 min after incubation with fluorescein isothiocyanate-conjugated LPS (FITC-LPS) was measured by flow cytometry. Data from each group were compared with those from the lipopolysaccharide (LPS) group and are expressed as ratios of mean fluorescence intensity (MFI). **b** Expression of membrane-bound CD14 at 60 min after LPS stimulation was measured by flow cytometry. Data from each group were compared with those from the lipopolysaccharide (LPS) group and are expressed as ratios of CD14-

positive events. **c** Levels of soluble CD14 at 60 min after LPS stimulation were measured by enzyme-linked immunosorbent assay. LPS, the lipopolysaccharide (1 $\mu\text{g}/\text{mL}$) group; LPS+M20, the LPS plus MgSO_4 (20 mM) group; LPS+M20+PMSF, the LPS plus MgSO_4 (20 mM) plus phenylmethanesulfonyl fluoride (PMSF, a mixed serine protease inhibitor, 0.4 mM) group. LPS+M20+EGTA, the LPS plus MgSO_4 (20 mM) plus ethylene glycol tetraacetic acid (a metalloproteinase inhibitor, 1 mM) group. Data are presented as mean \pm standard deviation ($n=6$ in each group). # $P<0.05$ for the LPS+M20 group versus the LPS group, ¶ $P<0.05$ for the LPS+M20+PMSF group versus the LPS+M20 group

Discussion

Findings from this study, in concert with those from previous studies (Gao et al. 2013; Sugimoto et al. 2012; Lin et al. 2010), confirm the potent anti-inflammatory effects of MgSO_4 . MgSO_4 decreased the level of IL-1 β , which is the key pro-inflammatory cytokine released in response to LPS stimulation (Lopez-Castejon and Brough 2011). Moreover, this study provides new insight into the mechanism mediating the anti-inflammatory effect of MgSO_4 , demonstrating that MgSO_4 may decrease binding of LPS to macrophages. We found that MgSO_4 may act through reducing CD14 expression via inhibiting CD14 upregulation (in both transcriptional and translational levels) and enhancing CD14 shedding to decrease LPS–macrophage binding, followed by decreased cytokine production. This concept is supported by previous data that overexpression of mCD14 results in hyper-responsiveness to LPS (Ferrero et al. 1993), whereas reduced levels of mCD14 cause hypo-responsiveness to LPS and an attenuation of proinflammatory cytokine release (LeBarillec et al. 1999, 2000; Sugawara et al. 2000; Tada et al. 2002). This study provides clear evidence to confirm the effects of MgSO_4 on inhibiting LPS binding to inflammatory cells. Endotoxin-bound immune cells are detected and play important roles in patients of various inflammatory diseases, such as gram-negative sepsis (Takeshita et al. 1999, 2000). In line with this concept, we thus believe that incorporating

MgSO_4 in the clinical therapies against endotoxin-related inflammatory diseases can be a novel therapeutic strategy. Data from this study thus should have profound clinical implications and warrant further investigation.

Furthermore, our previous study has demonstrated that antagonism of the L-type calcium channels is one crucial mechanism in mediating the anti-inflammatory effects of MgSO_4 (Lin et al. 2010). Data from this study show that the potent L-type calcium channel activator Bay-K8644 may counteract the effects of MgSO_4 on inhibiting LPS–macrophage binding and decreasing mCD14 upregulation, confirming the involvement of the L-type calcium channels in mediating the aforementioned effect of MgSO_4 . As MgSO_4 may act through antagonizing the L-type calcium channels to decrease intracellular calcium, we thus also investigated the changes in intracellular calcium levels in this study. Our data showed that the changes in intracellular calcium levels correlate well with those changes in LPS–macrophage binding and mCD14 upregulation. These data indicate that MgSO_4 may act by antagonizing the L-type calcium channels and decreasing intracellular calcium levels to inhibit CD14 upregulation. This concept is supported by previous data that LPS-induced transcription of CD14 involves activation of protein kinase C (PKC) and PKC activation is calcium-dependent (Hopkins et al. 1995; Landmann et al. 1996; Pedrinaci et al. 1990; Sun and Zemel 2008). Furthermore,

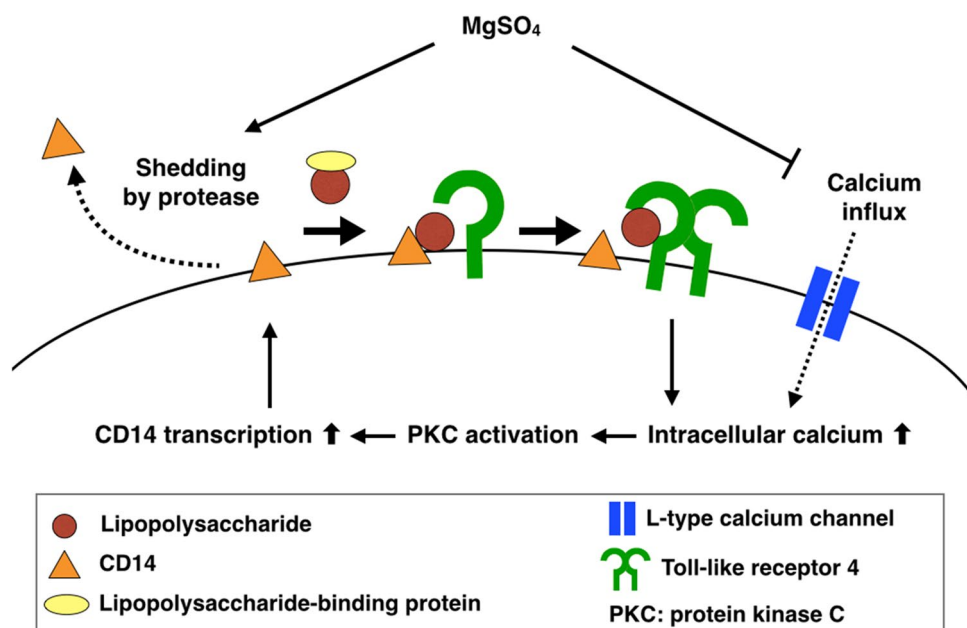


Fig. 7 Hypothesized mechanism underlying effects of magnesium sulfate ($MgSO_4$) on inhibiting lipopolysaccharide (LPS)–macrophage binding and reducing cluster of differentiation 14 (CD14) expression. $MgSO_4$ may reduce the level of intracellular calcium through antagonism of the L-type calcium channels and downregulate calcium-dependent protein kinase C activation-induced CD14 expression.

$MgSO_4$ may also enhance proteolytic cleavage of CD14 (i.e., CD14 shedding) by serine proteases to reduce membrane-bound CD14 (mCD14) expression. Both these mechanisms contribute to reducing the levels of mCD14 and downregulating CD14-dependent binding of LPS to macrophages

some L-type calcium channel blockers are demonstrated to downregulate CD14 expression in previous study (Sun and Zemel 2008). More studies are needed before further conclusions can be drawn.

Notably, the effect of $MgSO_4$ on enhancing CD14 shedding was not counteracted by L-type calcium channel activation. These data seem to suggest the involvement of mechanism(s) other than the L-type calcium channels or intracellular calcium in this regard. Previous studies have indicated that sCD14 is the proteolytic cleavage product of CD14, and proteolytic cleavage of CD14 is mediated by serine proteases or metalloproteinases (Le-Barillec et al. 1999, 2000; Pham 2008; Senft et al. 2005). Our data further demonstrate that the enhancement of CD14 proteolytic cleavage that was facilitated by $MgSO_4$ can be reversed by inhibition of serine proteases, indicating that $MgSO_4$ may act by activating serine proteases to enhance the proteolytic cleavage of CD14. This concept is supported by previous data that magnesium is crucial for maintaining activity of some proteases (Dong et al. 2008; Su et al. 2016). However, the question of whether serine proteases related to CD14 shedding, such as cathepsin G and human leukocyte elastase, are involved in mediating the effect of $MgSO_4$ remains unstudied. Furthermore, our data seemed to indicate that metalloproteinase are not involved in the effect of $MgSO_4$. Nonetheless, since only EGTA was used as the metalloprotease inhibitor in

this study, employment of various metalloprotease inhibitors (e.g., phosphoramidon) may provide more information.

Collectively, our results confirm that $MgSO_4$ inhibits LPS–macrophage binding by reducing CD14 expression. The mechanisms underlying the effects of $MgSO_4$ on reducing CD14 expression may involve blocking the L-type calcium channels and decreasing intracellular calcium as well as enhancing CD14 proteolytic cleavage via activating serine proteases. Our hypothesized mechanisms are illustrated in Fig. 7.

We acknowledge that although our results are clear, this study has certain limitations. First, the incubation period with LPS in most of the assays was limited to at most 60 min and only one dose of LPS (1 $\mu g/mL$) was employed. The effects of $MgSO_4$ on CD14 expression over long LPS incubation periods or under different doses of LPS have not been determined. Second, sCD14 can be generated through a mechanism other than proteolytic cleavage of mCD14, such as secretion of CD14 by the cells (Bufler et al. 1995). The effect of $MgSO_4$ on CD14 secretion was not examined in this study. In addition, reduced CD14 levels may result from an overall reduction in inflammatory responses as Bay-K8644 did not completely reverse the effect of $MgSO_4$ on mCD14 in our study. Third, CD14 is part of a receptor complex including LPS-binding protein (LBP) and TLR4. The effects of $MgSO_4$ on modulating LBP, TLR4, or other TLR4 complex

proteins remain unstudied in this investigation. Finally, the limited cell line employed in this study restricts the *in vivo* relevance. Future studies employing other “relevant” macrophage populations, such as primary macrophages, may provide further information in this regard.

In summary, MgSO₄ inhibits binding of LPS to macrophages by reducing CD14 expression. The mechanisms may involve antagonism of the L-type calcium channels and enhancing the activity of serine proteases.

Acknowledgements The authors thank Ms. Tai-Hsin Chang and Ms. Ching-Yun Chang for their excellent laboratory technical assistance. This study was supported by a grant from the Ministry of Science and Technology, Taiwan (MOST 105-2314-B-303-001-MY3), awarded to CJH.

Author contributions YYC and CJH contributed to the study concept and design; data collection, analysis, and interpretation; and writing and critical revision of the article. TYL, MCK, TYC, CFC, and CSW contributed to data analysis and interpretation as well as writing and critical revision of the article.

References

- Ahmed LA (2012) Protective effects of magnesium supplementation on metabolic energy derangements in lipopolysaccharide-induced cardiotoxicity in mice. *Eur J Pharmacol* 694(1–3):75–81
- Bufler P, Stiegler G, Schuchmann M, Hess S, Kruger C, Stelter F et al (1995) Soluble lipopolysaccharide receptor (CD14) is released via two different mechanisms from human monocytes and CD14 transfectants. *Eur J Immunol* 25(2):604–610
- Cai C, Shi X, Korff S, Zhang J, Loughran PA, Ruan X et al (2013) CD14 contributes to warm hepatic ischemia-reperfusion injury in mice. *Shock* 40(2):115–121
- Chen CP, Tsai PS, Huang CJ (2012) Anti-inflammation effect of human placental multipotent mesenchymal stromal cells is mediated by prostaglandin E2 via a myeloid differentiation primary response gene 88-dependent pathway. *Anesthesiology* 117(3):568–579
- Chen Z, Shao Z, Mei S, Yan Z, Ding X, Billiar T, Li Q (2018) Sepsis upregulates CD14 expression in a MyD88-dependent and Trif-independent pathway. *Shock* 49(1):82–89
- Chmielinska JJ, Tejerro-Taldo MI, Mak IT, Weglicki WB (2005) Intestinal and cardiac inflammatory response shows enhanced endotoxin receptor (CD14) expression in magnesium deficiency. *Mol Cell Biochem* 278(1–2):53–57
- Dong JF, Cruz MA, Aboufatova K, Martin C, Choi H, Bergeron AL et al (2008) Magnesium maintains endothelial integrity, up-regulates proteolysis of ultra-large von Willebrand factor, and reduces platelet aggregation underflow conditions. *Thromb Haemost* 99(3):586–593
- El-Tanbouly DM, Abdelsalam RM, Attia AS, Abdel-Aziz MT (2015) Pretreatment with magnesium ameliorates lipopolysaccharide-induced liver injury in mice. *Pharmacol Rep* 67(5):914–920
- Ferrero E, Jiao D, Tsuberi BZ, Tesio L, Rong GW, Haziot A et al (1993) Transgenic mice expressing human CD14 are hypersensitive to lipopolysaccharide. *Proc Natl Acad Sci USA* 90:2380–2384
- Gao F, Ding B, Zhou L, Gao X, Guo H, Xu H (2013) Magnesium sulfate provides neuroprotection in lipopolysaccharide-activated primary microglia by inhibiting NF- κ B pathway. *J Surg Res* 184(2):944–950
- Hopkins HA, Monick MM, Hunninghake GW (1995) Lipopolysaccharide upregulates surface expression of CD14 on human alveolar macrophages. *Am J Physiol* 269(6Pt1):L849–L854
- Kew KM, Kirtchuk L, Michell CI (2014) Intravenous magnesium sulfate for treating adults with acute asthma in the emergency department. *Cochrane Database Syst Rev* 5:CD010909
- Landmann R, Knorf HP, Link S, Sansano S, Schumann R, Zimmerli W (1996) Human monocyte CD14 is upregulated by lipopolysaccharide. *Infect Immun* 64(5):1762–1769
- Le-Barillec K, Si-Tahar M, Balloy V, Chignard M (1999) Proteolysis of monocyte CD14 by human leukocyte elastase inhibits lipopolysaccharide-mediated cell activation. *J Clin Investig* 103(7):1039–1046
- Le-Barillec K, Pidard D, Balloy V, Chignard M (2000) Human neutrophil cathepsin G down-regulates LPS-mediated monocyte activation through CD14 proteolysis. *J Leukoc Biol* 68(2):209–215
- Lee MY, Huang CH, Kuo CJ, Lin CL, Lai WT, Chiou SH (2015) Clinical proteomics identifies urinary CD14 as a potential biomarker for diagnosis of stable coronary artery disease. *PLoS One* 10(2):e0117169
- Lin CY, Tsai PS, Hung YC, Huang CJ (2010) L-type calcium channels are involved in mediating the anti-inflammatory effects of magnesium sulphate. *Br J Anaesth* 104(1):44–51
- Lopez-Castejon G, Brough D (2011) Understanding the mechanism of IL-1 β secretion. *Cytokine Growth Factor Rev* 22(4):189–195
- Ma L, Wu X-Y, Zhang L-H, Chen W-M, Uchiyama A, Mashimo T et al (2013) Propofol exerts anti-inflammatory effects in rats with lipopolysaccharide-induced acute lung injury by inhibition of CD14 and TLR4 expression. *Braz J Med Biol Res* 46(3):299–305
- Ma S, Chen C, Cao T, Bi Y, Zhou J, Li X et al (2017) Mitigation effect of proanthocyanidin on secondary heart injury in rats caused by mechanical trauma. *Sci Rep* 7:44623
- Molteni M, Gemma S, Rossetti C (2016) The role of Toll-like receptor 4 in infections and noninfectious inflammation. *Mediat Inflamm* 2016:6978936
- Park BS, Lee JO (2013) Recognition of lipopolysaccharide pattern by TLR4 complexes. *Exp Mol Med* 45:e66
- Pedrinaci S, Ruiz-Cabello F, Gomez O, Collado A, Garrido F (1990) Protein kinase C-mediated regulation of the expression of CD14 and CD11/CD18 in U937 cells. *Int J Cancer* 45(2):294–298
- Pham CT (2008) Neutrophil serine proteases fine-tune the inflammatory response. *Int J Biochem Cell Biol* 40(6–7):1317–1333
- Prestigiacomo V, Weston A, Messner S, Lampart F, Suter-Dick L (2017) Pro-fibrotic compounds induce stellate cell activation, ECM-remodelling and Nrf2 activation in a human 3D-multicellular model of liver fibrosis. *PLoS One* 12(6):e0179995
- Rosadini CV, Kagan JC (2017) Early innate immune responses to bacterial LPS. *Curr Opin Immunol* 44:14–19
- Senft AP, Korfhagen TR, Whitsett JA, Shapiro SD, Levine AM (2005) Surfactant protein-D regulates soluble CD14 through matrix metalloproteinase-12. *J Immunol* 174(8):4953–4959
- Shin MK, Shin SW, Jung M, Park H, Park HE, Too HS (2015) Host gene expression for *Mycobacterium avium* subsp. paratuberculosis infection in human THP-1 macrophages. *Pathog Dis* 73(5):ftv031
- Sonna LA, Hirshman CA, Croxton TL (1996) Role of calcium channel blockade in relaxation of tracheal smooth muscle by extracellular Mg²⁺. *Am J Physiol* 271(2 Pt 1):L251–L257
- Su SC, Lin CC, Tai HC, Chang MY, Ho MR, Babu CS et al (2016) Structural basis for the magnesium-dependent activation and hexamerization of the Lon AAA+ protease. *Structure* 24:676–686
- Sugawara S, Nemoto E, Tada H, Miyake K, Imamura T, Takada H (2000) Proteolysis of human monocyte CD14 by cysteine proteinases (gingipains) from *Porphyromonas gingivalis* leading to lipopolysaccharide hyporesponsiveness. *J Immunol* 165(1):411–418

- Sugimoto J, Romani AM, Valentin-Torres AM, Luciano AA, Ramirez Kitchen CM, Funderburg N et al (2012) Magnesium decreases inflammatory cytokine production: a novel innate immunomodulatory mechanism. *J Immunol* 188(12):6338–6346
- Sun X, Zemel MB (2008) Calcitriol and calcium regulate cytokine production and adipocyte-macrophage cross-talk. *J Nutr Biochem* 19(6):392–399
- Tada H, Sugawara S, Nemoto E, Takahashi N, Imamura T, Potempa J, Travis J, Shimauchi H, Takada H (2002) Proteolysis of CD14 on human gingival fibroblasts by arginine-specific cysteine proteinases from *Porphyromonas gingivalis* leading to down-regulation of lipopolysaccharide-induced interleukin-8 production. *Infect Immun* 70(6):3304–3307
- Takeshita S, Nakatani K, Kawase H, Seki S, Yamamoto M, Sekine I et al (1999) The role of bacterial lipopolysaccharide-bound neutrophils in the pathogenesis of Kawasaki disease. *J Infect Dis* 179(2):508–512
- Takeshita S, Nakatani K, Tsujimoto H, Kawamura Y, Seki I (2000) Detection of circulating lipopolysaccharide-bound monocytes in children with gram-negative sepsis. *J Infect Dis* 182(5):1549–1552
- Troelstra A, Antal-Szalmas P, de Graaf-Miltenburg LA, Weersink AJ, Verhoef J, Van Kessel KP et al (1997) Saturable CD14-dependent binding of fluorescein-labeled lipopolysaccharide to human monocytes. *Infect Immun* 65(6):2272–2277
- Weglicki WB, Mak IT, Chmielinska JJ, Tejero-Taldo MI, Komarov A, Kramer JH (2010) The role of magnesium deficiency in cardiovascular and intestinal inflammation. *Magnes Res* 23(4):S199–S206
- Wei Y, Chen J, Hu Y, Lu W, Zhang X, Wang R, Chu K (2018) Rosmarinic acid mitigates lipopolysaccharide-induced neuroinflammatory responses through the inhibition of TLR4 and CD14 expression and NF- κ B and NLRP3 inflammasome activation. *Inflammation* 41(2):732–740
- Zhu T, Zhang L, Ling S, Duan J, Qian F, Li Y et al (2014) Scropolioside B inhibits IL-1 β and cytokines expression through NF-kappaB and inflammasome NLRP3 pathways. *Mediat Inflamm* 2014:819053

Publisher's Note Springer Nature remains neutral with regard to jurisdictional claims in published maps and institutional affiliations.